Local bonding structure of Sb on Si(111) by surface extended x-ray-absorption fine structure and photoemission

J. C. Woicik
National Institute of Standards and Technology, Gaithersburg, Maryland 20899

T. Kendelewicz and K. E. Miyano
Stanford Electronics Laboratory, Stanford, California 94305

C. E. Bouldin
National Institute of Standards and Technology, Gaithersburg, Maryland 20899

P. L. Meissner, P. Pianetta, and W. E. Spicer
Stanford Electronics Laboratory, Stanford, California 94305
(Received 20 July 1990)

The combined techniques of surface extended x-ray-absorption fine structure (SEXAFS) and high-resolution core and valence photoelectron spectroscopy have been used to study the local bonding structure of the Sb/Si(111) interface. From photoemission, we find that the Sb atoms adsorb in a unique environment that completely saturates the dangling bonds of the Si(111) surface and that completely eliminates the surface components of the Si $2p$ core-level spectrum. The Sb-induced Si $2p$ interfacial core level is found to be shifted 0.20 ± 0.02 eV towards higher binding energy with an intensity that corresponds to the top monolayer of surface atoms. The SEXAFS determination of the absolute surface coordination numbers and bond lengths within the first Sb shell is 2.1 ± 0.3 Sb atoms at 2.86 ± 0.02 Å and 2.0 ± 0.4 Si atoms at 2.66 ± 0.03 Å. Combined, these results indicate that Sb trimers occupy the threefold atop sites of the Si(111) surface, where each Sb atom is bonded to two Si atoms in a modified bridge configuration.

INTRODUCTION

Understanding the metal-semiconductor interface has been a central issue confronting the surface-science community. This emphasis has arisen primarily from the importance of Schottky-barrier formation. Unfortunately, a large number of key issues remains unsolved in part due to the lack of knowledge of the adsorption geometry during the early stages of interface formation. From photoemission and other studies it is known that electronic properties of interfaces are often established at submonolayer to monolayer coverages. In this work we have combined the techniques of surface extended x-ray-absorption fine structure (SEXAFS) and high-resolution core and valence photoelectron spectroscopy (PES) to the study of the Sb/Si(111) interfacial structure. The advantages of combining these techniques arise from their complementary sensitivities: SEXAFS is a probe of surface geometric structure, and PES is a probe of surface electronic structure. By combining both techniques to the study of the same system, a rather complete structural determination is possible. In fact, as this study will show, due to the complementary nature of electronic and geometric structures, both sets of information are needed for an unambiguous determination of the adsorption site geometry. Furthermore, since Sb is weakly reactive with the Si surface, this study should serve to elucidate the role of geometric structure in Schottky-barrier formation as opposed to the role of chemistry in the more reactive metal-semiconductor interfaces.

Other studies pertinent to this work have been performed. In a PES study, Rich *et al.*[1] examined the electronic properties of the Sb passivated Si(111) surface. Unfortunately, the chemical shift of the Si $2p$ core level due to the Sb bonding was not resolved. Recently, we have demonstrated that accurate knowledge of the core-level line shape can lead to a precise determination of surface core-level shifts. The technique was demonstrated for the two prototypical semiconductor surfaces Si(111)2×1 (Ref. 2) and InP(110)1×1.[3]

This current work extends our method to the study of metal-semiconductor systems. As will be seen, accurate knowledge of the core-level line shape can lead to a unique deconvolution of core-level data whose shifts are significantly less than the total experimental resolution.

Recently, Abukawa, Park, and Kono[4] have used x-ray photoelectron diffraction (XPD) to study the geometric structure of the Sb/Si(111) interface. From the consideration of valency of the adatoms, it was tentatively inferred that Sb adsorbs in a "milk-stool" structure forming trimers which occupy the Si(111) $\sqrt{3}\times\sqrt{3}R\,30°$ threefold sites. However, neither the Sb—Si bond length nor the registry of the Sb trimers with the Si substrate could be determined from the XPD patterns. The most readily available structural parameters from a SEXAFS study are the adsorbate–surface atom bond length and the

adsorbate–surface atom coordination number, which are exactly those needed to unambiguously determine the structure implied in the XPD work. As will be seen, due to the properties of the Sb—Sb and Sb—Si bonds, the "milk-stool" geometry inferred by Abukawa, Park, and Kono,[4] where each Sb atom is bonded to only one Si atom, must be modified to accomodate the nondirectional close packing of covalent metallic atoms. Use of the polarization dependence of the L_1 and L_3 absorption edges in the determination of this surface structure will also be discussed.

EXPERIMENTAL

PES data were collected on beamline U16B at the National Synchrotron Light Source (NSLS) using an extended-range grasshopper (ERG) monochromator. The spectra were recorded at photon energies $h\nu=80$, 110, and 150 eV by use of a double-pass cylindrical-mirror analyzer (CMA) operating with Auger-electron spectroscopy (AES) slits. The pass energy was 5 and 25 eV for the core and valence measurements, respectively. The synchrotron radiation's polarization vector, $\boldsymbol{\varepsilon}$, was aligned 10° from the sample's normal, $\mathbf{n}$, which was parallel to the CMA axis (glancing incidence, $\boldsymbol{\varepsilon}\|\mathbf{n}$). The Fermi level at 80 eV was determined by measuring the valence-band spectrum from a freshly evaporated Ag film. The Sb/Si(111) interface was prepared by cleaving a 5-mm by 5-mm bar of lightly doped n-type single-crystal Si and evaporating 2 monolayers (ML) of Sb from a thoroughly degassed W coil. The sample was then annealed for 15 min at 375 °C. Since the sticking coefficient of Sb to itself is zero at this temperature,[5] this procedure was chosen to ensure that the Si surface was saturated with a full monolayer of Sb atoms. The evaporation rate was calibrated by a quartz crystal balance and cross checked by photoemission. The base pressure of the vacuum chamber was better than 1.5×10^{-10} Torr.

SEXAFS data were collected on beamline X15B, also at NSLS, using a fixed exit double-crystal monochromator operating with a pair of Ge(111) crystals. The experiment was conducted in the same vacuum chamber as used in the photoemission experiment. The sample photocurrent was measured as a function of incident photon energy and flux as the photon energy was scanned across the Sb L_3 ($h\nu=4132$ eV) and L_1 ($h\nu=4698$ eV) absorption edges. The incident flux was taken as the photocurrent from an 80% transmission Ni grid upstream of the sample. Data were recorded at normal ($\boldsymbol{\varepsilon}\perp\mathbf{n}$), glancing ($\boldsymbol{\varepsilon}\|\mathbf{n}$), and, as will be discussed later, the "magic" angle, 54.7° from glancing, ($\boldsymbol{\varepsilon}\angle\mathbf{n}$) incidence. Sample preparation was the same as that used in the photoemission experiment, but the initial Sb coverage was somewhat less, 1.2 ML, in order to avoid the possible contribution from Sb clusters to the SEXAFS spectra. Low-energy electron diffraction (LEED) shows a sharp 1×1 pattern with some diffuse higher-order spots for this sample preparation procedure. The Sb EXAFS standard was recorded in total yield from a freshly evaporated Sb film, and the AlSb EXAFS standard was recorded in transmission from a freshly ground AlSb powder.

RESULTS

A. PES

Figure 1 shows the valence-band spectrum from the Sb/Si(111) interface. Indicated in the figure is the Fermi level as determined from the Ag film. These data were recorded with photon energy $h\nu=80$ eV. By extrapolating the valence-band maximum to zero intensity, it is clear that the position of the valence-band maximum lies approximately 1 eV below the Fermi level. Since the band gap of Si is 1.12 eV, as reported by other workers,[1] the adsorption of a monolayer of Sb atoms results in a flat band condition where the Fermi level lies at the bottom of the conduction band for an n-type sample. Originally, the Si surface Fermi level is pinned about a third of the way up from the valence- to the conduction-band edges due to the presence of the Si(111) dangling-bond states in the band gap.[6] In order for a flat band condition to arise, all of the Si dangling bonds must be saturated, and the Si surface states removed from the band gap.

Figure 2 shows the Sb 4d core level from the Sb/Si(111) interface taken with photon energy $h\nu=80$ eV. Shown also in the figure is the result of a two-singlet least-squares fit to the data. The solid line is the fit, and the dots are the data points. In this spectrum, an integrated background, which is assumed to account for inelastic processes,[7] has been removed prior to the curve fitting. The two singlets represent the spin-orbit split components of the Sb 4d core level; they are the convolution of a Gaussian, which represents the experimental width, and a Lorentzian, which accounts for the lifetime of the core hole.[8] This procedure gave a Gaussian width equal to 0.396 eV and a Lorentzian width equal to 0.187 eV. The spin-orbit splitting, which is the energy seperation of the two singlets, and the branching ratio, which is the ratio of their intensities, are found to be 1.25 eV and 1.47, respectively. The spin-orbit splitting and the Lorentzian width are in close agreement with those reported by Rich *et al.*,[1] and the branching ratio is close to the statistical value of 1.5 for d states. As can be seen, the quality of the fit is excellent, and we take the resulting doublet to accurately represent the Sb 4d core-level line shape.

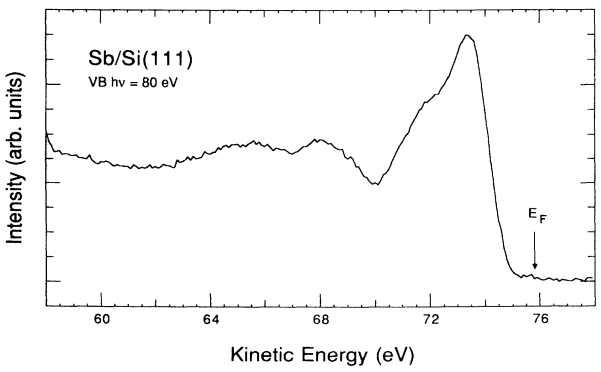

FIG. 1. The valence-band spectrum from the Sb/Si(111) interface taken with photon energy $h\nu=80$ eV. Marked in the figure is the Fermi level as determined from the Ag film.

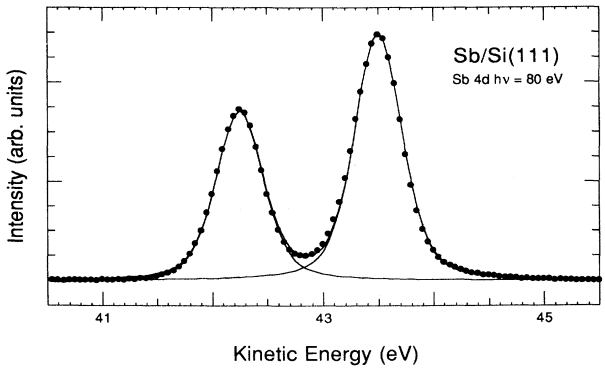

FIG. 2. The background-corrected Sb 4*d* core-level spectrum from the Sb/Si(111) interface taken with photon energy $h\nu=80$ eV. Shown in the figure is the least-squares fit (solid line) to the data points.

Since the Sb core level from the annealed surface is so well represented by one doublet with two components of equal width, we may conclude that each Sb atom is adsorbed in a unique environment, i.e., there is no multisite adsorption. Had Sb atoms existed in more than one environment, more than one Sb core-level component would exist.[9] For example, core levels derived from Sb atoms bonded to Sb atoms in three-dimensional clusters and also from Sb atoms which have diffused into the Si substrate would contribute to the spectrum. Since we observe only one distinct Sb core level, we may conclude that this core level originates from Sb atoms which are bonded to Si atoms at the Sb/Si(111) interface.

Figures 3(a) and 3(b) show the Si 2*p* core level from the Sb/Si(111) interface taken with photon energies $h\nu=110$ and 150 eV. These photon energies were chosen to maximize ($\lambda\sim12$ Å) and minimize ($\lambda\sim5$ Å) the escape depth of the photopeak.[10] In each case, the figures show a two-doublet least-squares fit to the data. Once again, the solid lines are the fits, and the dots are the data points. Each spectrum has had an integrated background removed prior to the curve fitting. The spectrum taken at photon energy $h\nu=110$ eV has also had an additional inelastic background, which is due to higher-energy electrons, removed. This additional inelastic background was measured over the same kinetic-energy region as the photopeak, but it was taken with photon energy $h\nu=100$ eV in order to remove the photopeak from the kinetic-energy window.

For the bulk sensitive spectrum recorded at photon energy $h\nu=110$ eV, the line shape of the two doublets used in the curve-fitting procedure was determined by fitting two singlets to the Si 2*p* core-level spectrum from a Bi-covered Si(111) surface recorded at the same photon energy. The line shape from the Bi-covered surface was used since the Si core levels from this interface were narrower than those from the Sb-covered surface in accord with the smaller electronegativity difference between Bi-Si and Sb-Si pairs.[11] The results of the Bi/Si(111) experiment, which provide a good estimate of the intrinsic Si 2*p* line shape, will be presented at a later date. This fitting procedure gave a Gaussian width equal to 0.303 eV and a Lorentzian width equal to 0.078 eV. The spin-orbit splitting and the branching ratio were found to be 0.607 eV and 2.02, respectively. These line-shape parameters are similar to those which we determined from a Ge-covered Si(111) surface,[2] and the branching ratio is close to the statistical value of 2 for *p* states.

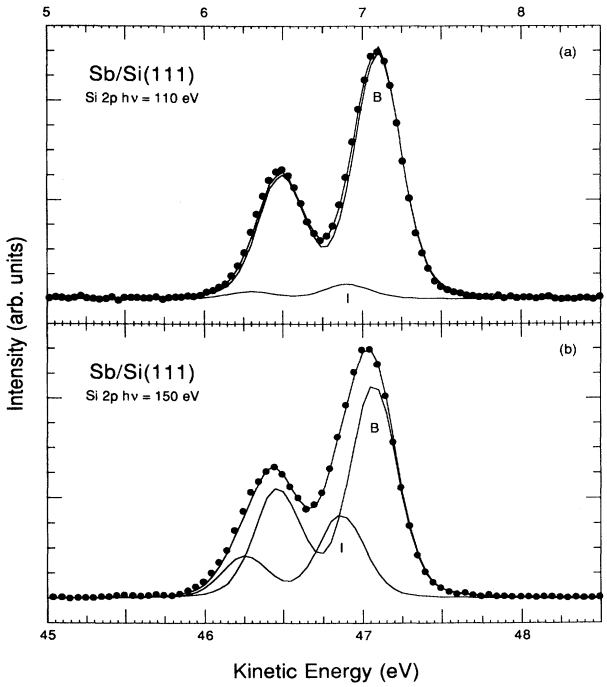

FIG. 3. The background-corrected Si 2*p* core-level spectrum from the Sb/Si(111) interface taken with (a) photon energy $h\nu=110$ eV and (b) photon energy $h\nu=150$ eV. Shown in the figures are the least-squares fits (solid lines) to the data points. The Sb-induced interfacial core level is marked *I*, and the bulk peak is marked *B*.

Comparison of the Bi 5*d* spectra recorded at photon energies $h\nu=110$ and 150 eV showed that the monochromator resolution was slightly better at photon energy $h\nu=150$ eV. Since an interfacial component from the Bi-covered Si(111) surface obscured the determination of the Gaussian width at the surface-sensitive photon energy of $h\nu=150$ eV, we chose a Gaussian width of 0.300 eV for the deconvolution of the surface-sensitive spectrum from the Sb-covered surface. We also determined the actual photon energy difference between the two monochromator settings; it was 40.5 ± 0.05 eV. The two spectra in Fig. 3 have been shifted in energy by exactly this amount.

Since other workers[1] failed to resolve an interfacial Si 2*p* component, it is important to stress that evidence for the existence of such a shift comes from visual inspection of the data alone. First, since we have determined that the experimental resolution at photon energy $h\nu=150$ eV is better than the experimental resolution at photon energy $h\nu=110$ eV, the greater width of the more surface sensitive Si 2*p* spectrum indicates that there is additional intensity coming from the surface region which is shifted

relative to the bulk. Second, it is evident that the peak position of the surface-sensitive spectrum is displaced by approximately 0.15 eV towards lower kinetic energy relative to the peak position of the bulk sensitive spectrum. Further, when we attempted to fit the surface-sensitive spectrum with two singlets, we found the width of the lower kinetic-energy $2p_{1/2}$ component to be greater than the width of the higher kinetic-energy $2p_{3/2}$ component. This apparent asymmetry implies that the interfacial intensity lies at the low kinetic-energy side of the bulk peak. Our deconvolution procedure finds this interfacial component to be shifted 0.20 ± 0.02 eV towards lower kinetic energy with an intensity 0.39 ± 0.05 that of the bulk peak. The intensity of this component in the bulk sensitive spectrum is reduced to 0.06, in accord with the longer electron escape depth at the lower kinetic energy. The two components are labeled *I* and *B* for interface and bulk, respectively.

It is interesting to note that the electronegativity difference between Sb and Si is 0.15.[11] Therefore, we find the magnitude of the core-level shift to be close to the electronegativity difference between Sb and Si atoms. Such an empirical relation has been discussed previously by Himpsel *et al.*[12] for a wide range of adsorbates on Si.

It is instructive to estimate the number of Si atoms which contribute to the interfacial core-level shift. By adding the contribution from atomic planes along the [111] direction and assuming an escape depth of $\lambda=4.7$ Å (two nearest-neighbor distances for ease of calculation), it is straightforward to show that the contribution to the surface-sensitive PES spectrum from the first single monolayer of Si atoms would be 0.36 that of the remaining atoms. This result agrees quite well with our experimentally determined core-level intensity ratio of 0.39 ± 0.05.

B. XAFS

Figure 4 shows the Sb L_1 x-ray absorption near-edge structure from the Sb/Si(111) interface. These data were recorded at both normal ($\varepsilon\perp\mathbf{n}$) and glancing ($\varepsilon\|\mathbf{n}$) incidence. Also shown is the L_1 absorption spectrum from Sb metal. Note the strong polarization dependence of the data from the Sb monolayer, which, at normal incidence, resemble quite closely the data from the Sb metal. At normal incidence the $|\varepsilon\cdot\mathbf{r}|^2$ term of the EXAFS equation for absorption from initial *s*- to final *p*-like states[13] preferentially samples bonding from atoms which have their bond vector oriented parallel to the surface. At glancing incidence only bonds which have a component perpendicular to the surface are sampled. In the photoelectron diffraction work of Abukawa, Park, and Kono,[4] it was tentatively inferred that Sb trimers reside in the threefold sites of the Si(111) surface. For this geometry, L_1 absorption would preferentially sample Sb-Sb bonding when the polarization vector lies in the surface plane, i.e., normal incidence. When the polarization vector lies perpendicular to the surface, i.e., glancing incidence, only Sb-Si bonding would be sampled.

The feature near photon energy $h\nu=4730$ eV is the most sensitive to the sample orientation. This feature is

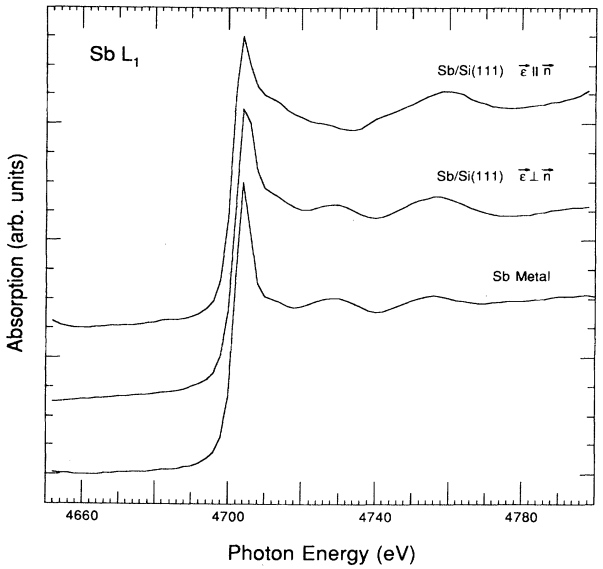

FIG. 4. The Sb L_1 x-ray adsorption near-edge structure from the Sb/Si(111) interface taken with the polarization vector ε aligned parallel (glancing incidence, $\varepsilon\|\mathbf{n}$) and perpendicular (normal incidence, $\varepsilon\perp\mathbf{n}$) to the [111] surface normal, $\mathbf{n}$. Also shown is the near-edge structure from Sb metal. Note the similarity (in particular the feature near $h\nu=4730$ eV) between the data from the Sb/Si(111) interface recorded at normal incidence and that from the Sb metal. This feature is absent in the data from the Sb monolayer recorded at glancing incidence.

the same as that of the Sb metal; it therefore originates from Sb backscattering. From this strong anisotropy, we may conclude that the Sb trimers reside parallel to the surface plane. Further, as was evident from our PES measurements, we may rule out three-dimensional Sb clustering since the presence of Sb clusters would lead to L_1 absorption with no polarization dependence. Analysis of the XPD patterns found the Sb-Sb bond length within the trimer to be 2.9 ± 0.1 Å.[4] This bond length is close to that of Sb metal, which is 2.87 Å.[14] From the energy position and intensity of this feature, it is clear that the properties of the surface Sb—Sb bond, i.e., the bond length and the coordination number, are comparable to those of bulk Sb.

Figure 5(a) shows the k^2-weighted Sb L_3 SEXAFS from the Sb/Si(111) interface recorded at the magic angle of 54.7° from glancing incidence ($\varepsilon\angle\mathbf{n}$). Although the data range of the L_3 edge is limited to 250 eV by the spin-orbit splitting of the initial *p* state, it has the greatest signal-to-background ratio of three *L* edges, and it lacks the residual low-frequency SEXAFS which contaminate the L_1 and L_2 edges.[15] For these reasons, we have chosen the L_3 absorption edge for our quantitative SEXAFS analysis. Superimposed on the raw data in Fig. 5(a) is the Fourier filtered first-shell contribution to the SEXAFS.

Figure 5(b) shows the fit to the first-shell signal assuming Sb-Sb and Sb-Si backscattering. The solid line is the fit, and the dots are the data points of the backtransform.

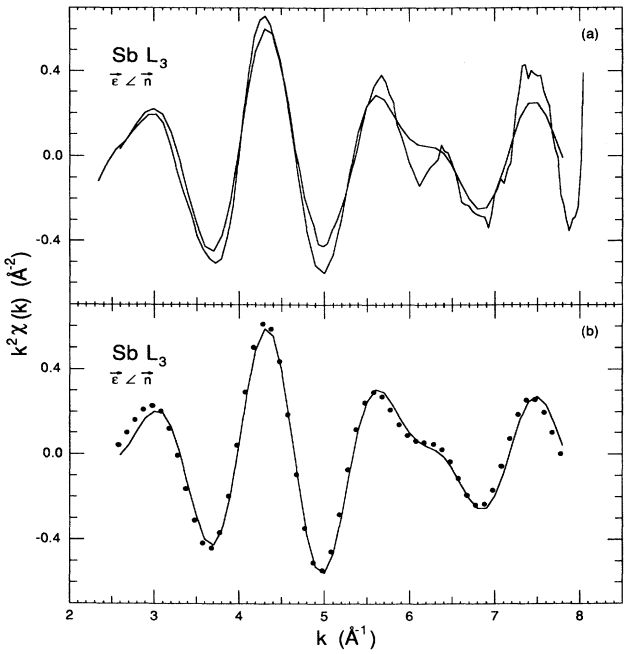

FIG. 5. (a) The k^2-weighted Sb L_3 SEXAFS from the Sb/Si(111) interface recorded at the magic angle ($\varepsilon \angle \mathbf{n}$) of 54.7° from glancing incidence. Superimposed on the data is the Fourier filtered first shell contribution to the SEXAFS. (b) The fit to the first shell signal assuming Sb-Sb and Sb-Si backscattering. The solid line is the fit, and the dots are the data points of the back transform. The values returned from the fit are 2.1±0.3 Sb atoms at 2.86±0.02 Å and 2.0±0.4 Si atoms at 2.66±0.03 Å.

The use of a two-component fit was motivated by the identification of Sb-Sb bonding in the L_1 near-edge structure. The presence of the two interfering components is also evident from the Fourier filtered data which shows a strong beating near $k = 6.3$ Å^{-1}. The Sb-Sb and Sb-Si components are closely represented by the experimentally determined EXAFS from Sb metal and crystalline AlSb, which have known structures. It is reassuring to see that even the beat is well modeled by the theoretical fit. The parameters determined from the fit are 2.1±0.3 Sb atoms at 2.86±0.02 Å and 2.0±0.4 Si atoms at 2.66±0.03 Å. Together, these coordination numbers and bond lengths indicate that Sb trimers occupy the threefold sites of the Si(111) surface. In this local bonding unit, each Sb atom is also bonded to two Si atoms.

In order to distinguish between the two adjacent threefold sites, i.e., either the threefold atop or the threefold hollow, it is necessary to have information on the second-neighbor distance which requires single-component data. Recall that the complex bonding properties of this interface give rise to a strong beating in the L_3 edge SEXAFS. For this reason we chose to examine the L_1 edge data recorded at glancing incidence ($\varepsilon \| \mathbf{n}$) more carefully. At glancing incidence, the L_1 absorption samples only Sb-Si bonding as was evident from the Sb L_1 near-edge structure.

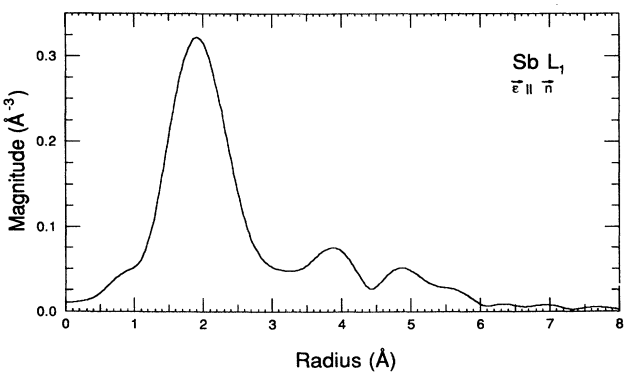

FIG. 6. The magnitude of the Fourier transform of the k^2-weighted Sb L_1 SEXAFS from the Sb/Si(111) interface recorded at glancing incidence ($\varepsilon \| \mathbf{n}$). The peak near 1.9 Å corresponds to the first shell Sb-Si bonding with bond length of 2.66±0.03 Å. The peak near 3.9 Å would correspond to second shell Sb-Si bonding with a bond length of 4.7±0.3 Å (see text).

Figure 6 shows the magnitude of the Fourier transform of the k^2-weighted Sb L_1 SEXAFS from the Sb/Si(111) interface recorded at glancing incidence ($\varepsilon \| \mathbf{n}$). The main peak near 1.9 Å corresponds to the first neighbor 2.66±0.03 Å Sb-Si bonding. If we account for the atomic phase shifts in the same way, the second peak in the transform would correspond to a second-neighbor Sb-Si distance of 4.7±0.3 Å. Such an extremely large second-neighbor distance implies an unphysically large, 1.5-Å, expansion in the distance between the first- and second-neighbor Si atoms. Even in the extreme case of the Ag/Si(111) $\sqrt{3}\times\sqrt{3}R30°$ structure where Ag atoms were found to adsorb between the first and second layer Si atoms, only a small, 0.3 Å, expansion between the first- and second-layer Si atoms was determined.[15] We therefore suggest that the Fourier peak near 3.9 Å corresponds to either of the two triangular multiple scattering pathways within the first Sb shell. These pathways occur between two Sb atoms and one Si atom or between one Sb atom and two Si atoms. They have half path lengths of 4.09±0.03 and 4.58±0.03 Å, respectively. Due to the difference in the slopes of the Sb and Si backscattering phase shifts, the Fourier positions of either may be reconciled with that observed in the transform. It is not surprising that second-neighbor distances are not observed in the Sb SEXAFS spectra. Comin *et al.*[16] attributed similar findings to vibrational damping between the substrate and higher Z (more weakly bound) adsorbates.

DISCUSSION

It has been know for some time that the surface atoms of clean single crystal surfaces move from their bulk positions in order to minimize their total energy.[6] These atomic displacements are referred to as surface reconstruction. The movement of the atoms may be a simple relaxation in the outermost layer as in the case of GaAs(110)1×1,[17] or it may be a complex arrangement in which the size of the surface unit cell becomes much

larger than that of the bulk surface as in the case of Si(111)7×7.[6] The π bonded chain model originally proposed by Pandey[18] for the Si(111)2×1 reconstruction differs from both of these cases in that the atoms of the first full double layer reconstruct to form two levels of quasi-one-dimensional zigzag chains which run along the $[1\bar{1}0]$ direction. The driving force for the reconstruction is the minimization of the number of dangling bonds which are produced upon cleaving.

For Si, the dangling bonds form a surface-state band which pins the Fermi level about a third of the way up the band gap between the valence- and the conduction-band edges.[6] A valence-band spectrum showing the position of these surface states relative to the Fermi level may be found in Ref. 2. In order for a flat band condition to arise, i.e., the surface Fermi level lying close to the conduction-band edge for an *n*-type sample, all of the dangling bonds must be saturated. Since the presence of the dangling bonds is the driving force for the reconstruction, an ideal 1×1 bulklike geometry may result, as, for example, in the case of the hydrogen terminated Si(111) surface where both the occupied[6] and unoccupied[19] surface states are removed from the band gap. It is important to mention that, despite massive rearrangment of atoms in going from a buckled to a chain geometry on the Si(111) surface, there is only a small, 0.03 eV, energy barrier between these two reconstructions.[20] The 2×1 reconstruction can therefore be easily relieved by the presence of the Sb overlayer.

Our observation of a flat band condition for the Sb/Si(111) interface poses a constraint on the structure which is consistent with the $\sqrt{3}\times\sqrt{3}R30°$ pattern observed by other workers,[21] i.e., all of the Si dangling bonds must be saturated. A 2×2 reconstruction, for example, has one dangling bond per unit cell, and it would therefore not result in a flat band condition. In order to preserve the $\sqrt{3}\times\sqrt{3}R30°$ translational symmetry in the presence of a full monolayer of adatoms, Lander and Morrison[22] hypothesized that trimers of adsorbates would occupy the threefold sites of the Si(111) surface. A picture of this reconstruction and others pertinent to the present work may also be found in Stohr *et al.*[15] In this model each dangling bond is saturated, and, unlike the case of monovalent hydrogen, it is the trimerization of the adsorbate atoms which results in the long-range $\sqrt{3}\times\sqrt{3}R30°$ periodicity.

In a recent photoemission study, we demonstrated that at least four components contribute to the surface-sensitive Si 2*p* core-level spectrum from the cleaved Si(111)2×1 surface.[2] These components were attributed to specific atoms involved in the reconstruction. In particular, two distinct core-level shifts originating from the two inequivalent atoms in the outermost chain were resolved. Apparently, these atoms exchange charge between themselves, which accounts for the buckling of the chains as determined by energy minimization.[20] This deconvolution was made possible by our accurate knowledge of the Si 2*p* core-level line shape which was determined from the core-level spectrum from a Ge-covered Si(111) surface. The most important aspect of photoemission pertinent to this work is its direct sensitivity to atoms in different electronic states. To this end, photoemission has been an indispensible tool for the study of solid surfaces and interfaces.

As we have determined, the Si 2*p* core level from the Sb-covered surface possesses an interfacial core level which is shifted 0.20±0.02 eV towards lower kinetic energy with an intensity 0.39±0.05 that of the remaining atoms. The significance of such a well-defined core-level shift is twofold. First, it is clear that the Sb atoms are only weakly reactive with the Si surface. Chemical reaction and the subsequent disruption of the surface results in a large number of core-level shifts due to the presence of many inequivalent chemical species. Our findings are more the exception to various metal-semiconductor interfaces than the rule.[23] Second, the presence of such a well-defined core-level shift implies that the Sb overlayer forms an ordered structure on the Si surface with the underlying Si atoms existing in an unreconstructed geometry. This last point is apparent since the core-level shifts associated with the different atoms of the Si(111)2×1 reconstruction are removed by the Sb overlayer. Assumptions such as these have often been made in the interpretation of SEXAFS data from semiconductors,[24] but they have seldom been experimentally justified. Further evidence of the overlayer order is given by the Sb core-level spectrum which shows only a single Sb component. In light of the present data, we may conclude that it is the Sb mosaic on the Si(111) surface which gives rise to the $\sqrt{3}\times\sqrt{3}R30°$ pattern rather than an underlying Si reconstruction. The intensity of the interfacial core level also implies that the interface is atomically abrupt since the Sb atoms are bonded to only the top monolayer of Si atoms.

It is useful to compare the magnitude of the Si 2*p* core-level shift to the Pauling electronegativity difference between Sb and Si atoms. This difference is 0.15, with the Sb atoms being the more electronegative;[11] it is close to the magnitude of the core-level shift observed in the Si 2*p* core-level spectrum, 0.20±0.02 eV. The fact that the Sb is the more electronegative atom explains why the interfacial core-level shift lies at the higher binding energy relative to the remaining Si atoms. Since charge transfer occurs in the direction of greater electronegativity, the Si surface atoms donate electron charge to the Sb atoms. An electron originating at a positively charged surface Si atom will require additional energy to escape this positive field, hence the increase in binding energy. The presence of such a small shift also implies that the bonding between Si and Sb has only a small ionic character; just a fraction of an electron charge is transferred from the Si to the Sb atoms. Other experimental work has found that, for small electronegativity difference, the magnitude of the adsorbate-induced Si core-level shift is roughly equal to the electronegativity difference multiplied by the number of adsorbed ligands per surface Si atom.[12] Interpretation of our data implies that, *on average,* there is approximately one Sb atom per first layer Si atom within a well-ordered structural unit. This constraint is to be coupled with our finding from the valence-band spectrum that all of the Si(111) dangling bonds are saturated by the Sb overlayer. Even more significantly, our PES measure-

ments show that the structural parameters deduced from our SEXAFS analysis may be interpreted in terms of the bulk Si structure, i.e., as the placement of Sb adatoms on the ideal Si(111)1×1 surface.

Having focused on the structural constraints obtained from photoemission, we now turn to the interpretation of our SEXAFS data. Figure 7 shows our structural model for the Sb/Si(111) local bonding unit based on the coordination numbers and bond lengths determined from the fit in Fig. 5(b). The sizes of the Sb and Si atoms have been scaled to their covalent radii.[11] Here Sb trimers occupy the threefold atop sites of the Si(111) surface where each Sb atom is bonded to two Si atoms. The presence of Sb trimers has been confirmed by our SEXAFS analysis since each Sb atom has two Sb near neighbors. Recall that the Sb L_1 near-edge structure found the Sb-Sb bonding to be parallel to the surface plane. In this structural unit, each Sb atom also has two Si near neighbors. We refer to this bonding scheme as a modified bridge configuration since the Sb atoms are shifted relative to the center of their Si neighbors, i.e., the bridge. The horizontal displacement from the center of the bridge is determined by the size of the Sb atoms; it is 0.54±0.02 Å. The vertical distance which the Sb atoms reside above the Si surface plane is $d_\perp = 1.76 \pm 0.03$ Å. In determining these distances, we have assumed that the distance between the first layer Si atoms in the threefold sites, i.e., the second-neighbor Si distance, 3.84 Å, has not been modified by the presence of the Sb trimers.

This structure is similar to the three-legged "milk-stool" geometry proposed by Abukawa, Park, and Kono[4] based on their XPD data, however, we find that the trimers are rotated 60° with respect to the Si substrate. We should mention that the XPD work could determine neither the Sb-Si bond length nor the registry of the Sb trimers with the Si substrate. The determination of the local bonding unit shown in Fig. 7 is a consequence of our direct determination of the *absolute* surface coordination numbers and bond lengths. It is interesting to find that the Sb-Sb distance is the same as that in Sb metal, 2.87 Å.[14] It is also interesting to find that the Sb-Si bond length is the same as that in AlSb, 2.66 Å.[25] These results indicate that the Sb—Sb bond is covalent, but the Sb—Si bond is slightly ionic. The degree of ionicity inferred from the similarity with the AlSb bond length is experimentally observed as an interfacial shift in the Si 2*p* core-level spectrum. The magnitude of the core-level shift is also in accord with the electronegativity difference between Sb-Si pairs. We conclude, therefore, that it is the nondirectional close packing of covalent metallic atoms which leads to the structure shown in Fig. 7, rather than the less tightly packed milk-stool structure proposed by Abukawa, Park, and Kono[4] which was based on valence arguments. In the milk-stool structure shown in Ref. 4, each Sb atom is bonded to only one Si atom. If the Sb atom had only one Si near neighbor, they would reside much further, $d_\perp = 2.52 \pm 0.03$ Å, from the Si substrate.

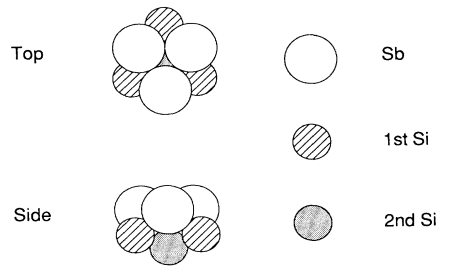

FIG. 7. Top and side view of the Sb/Si(111) local bonding unit derived from this work. Sb trimers occupy the $\sqrt{3}\times\sqrt{3}R30°$ threefold atop sites of the Si(111) surface. The relative sizes of the Sb and Si atoms have been scaled to their covalent radii.

As the bottom half of Fig. 7 shows, we have assigned the Sb trimers to occupy the threefold atop sites of the Si(111) surface. In the atop site, the Sb trimers occupy the threefold sites in which the second-neighbor Si atom lies directly beneath the center of the Sb trimer. This assignment is based on the consideration of the Fourier transform shown in Fig. 6 combined with our intuition concerning the radial distance of the second-neighbor Si atom. For this site, the polarization dependence of the L_1 edge reduces the contribution of the second-neighbor shell by 30%. Had the Sb trimers adsorbed in the adjacent threefold hollow sites, the second-neighbor Si atom would lie beneath the center of an Sb atom, and its signal would not be diminished in the Fourier transform. More significantly, if the Sb trimers resided in the site which we have ruled out, the distance between an Sb atom and a second-layer Si atom would be shorter than the distance between an Sb atom and a first-layer Si atom. The Sb-Si second-neighbor distance in the undistorted threefold atop site is 3.55±0.03 Å. This distance is close to the second-neighbor distance in pure crystalline Si, 3.84 Å; it is therefore a much more physical choice. The assignment of the threefold atop site is also the only site consistent with our photoemission data since we find that the Sb atoms are bonded to only the top one monolayer of Si atoms. The magnitude of the Si 2*p* core-level shift may also be reconciled with our assignment since, within the local bonding unit, there is one Sb atom for each Si atom.

This adsorption geometry is somewhat unusual in that the number of first near-neighbor Si atoms, 2, is greater than the number of second near-neighbor Si atoms, 1. It is therefore not surprising that a second shell signal is not observed in the SEXAFS spectra, for, even in the case of pure crystalline Si where there are 4 Si near neighbors and 12 second Si near neighbors, the second shell signal is down by a factor of 2 relative to that of the first shell in the Fourier transform due to inelastic effects.[26] From this property of Si backscattering, the contribution from the second Si shell in our surface data would be reduced by a factor of 12 relative to that of the first. Hence it would not be observable in the Fourier transform.

Traditionally, SEXAFS studies have focused on the bonding properties of isolated adsorbates on surfaces.[27] This study is a departure in that the first Sb shell here contains adsorbate atom–adsorbate atom first shell near-neighbor bonding. For this reason, we will illustrate the symmetry considerations which justify our use of the L_3

absorption edge data recorded at the magic angle to determine the *absolute* surface coordination numbers and bond lengths. This illustration is important because the polarization-dependent *relative* coordination numbers are not as tractable due to the presence of both Sb and Si backscattering within the first shell SEXAFS.

For K or L_1 edge absorption, the dipole selection rule, $\Delta l = \pm 1$, allows only $s \rightarrow p$ transitions, hence, the $|\boldsymbol{\varepsilon}\cdot\mathbf{r}|^2$ polarization term of the SEXAFS equation and the well-known "search-light" effect. For L_3 absorption, this anisotropy is reduced due to the symmetry of the initial p state. Stohr and Jaeger[28] have shown that the interference term between the two dipole-allowed $p \rightarrow s$ and $p \rightarrow d$ adsorption processes can lead to significant errors in the derived bond lengths and erroneous chemisorption geometries if standard analysis methods are applied. However, for the special case when the adsorption geometry possesses greater than twofold symmetry, they have shown that data recorded at the magic angle of 54.7° from glancing incidence are formally equivalent to the K or L_1 edge cases, and the bond lengths and coordination numbers may be determined directly by comparison with an isotropic model compound.

Figure 8(a) shows the top view of the structure determined by our combined photoemission and SEXAFS study. Note that this local bonding unit possesses a C_3 axis through the center of the Sb trimer. If we consider only the first shell SEXAFS, translational invariance allows us to decompose this structure into two subclasses of structures each of which has only one central absorbing Sb atom. The SEXAFS from the Sb-Sb bonding is equivalent to the SEXAFS from a central absorbing Sb atom which is surrounded by six backscattering Sb atoms. Figure 8(b) shows this structure, which is a planar sixfold hollow. This inherent sixfold symmetry about the central Sb atom accounts for the sixfold symmetry of the XPD patterns reported by Abukawa, Park, and Kono.[4] The SEXAFS from the Sb-Si bonding may be decomposed into the SEXAFS from the two structures shown in Fig. 8(c), both of which are threefold hollows. They have been rotated by ~28° with respect to each other about their C_3 axis. The Sb SEXAFS from structure (a) is formally equivalent to one-third the central Sb SEXAFS from structure (b) plus one-third the sum of the Sb SEXAFS from the two structures in (c). Since each of these structures possesses greater than twofold symmetry about the central axis, the criterion discussed by Stohr and Jaeger[28] is met, and we may analyze our L_3 edge data recorded at the magic angle as if it were a K or L_1 edge case.

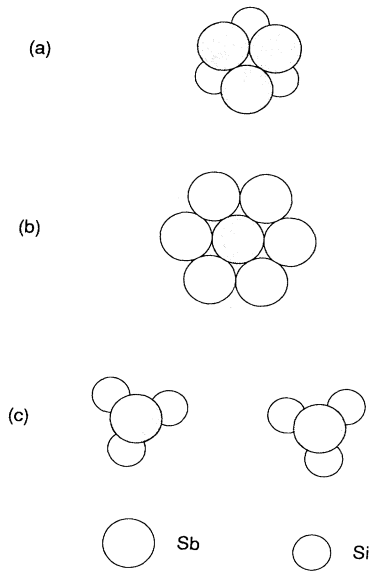

FIG. 8. Top view of (a) the Sb/Si(111) local bonding unit derived from this work, (b) a central absorbing Sb atom (shaded) bonded to six backscattering Sb atoms in a coplanar sixfold hollow, and (c) absorbing Sb atoms (shaded) bonded to three backscattering Si atoms in threefold hollows. The structures in (c) are rotated by ~28° about their vertical axis with respect to each other. Note that the Sb first shell SEXAFS from the structure in (a) is formally equivalent to the first shell SEXAFS from one-third the structure in (b) plus one-third the sum of the two structures in (c).

CONCLUSIONS

The combined techniques of surface extended x-ray absorption fine structure and high resolution core and valence photoelectron spectroscopy have been used to study the local bonding structure of the Sb/Si(111) interface. By combining the electronic information obtained from photoemission with the geometric parameters deduced from SEXAFS, a rather complete structural determination has been made.

From photoemission, we find that Sb atoms adsorb in a unique environment which completely saturates the dangling bonds of the Si(111) surface. Analysis of the Si $2p$ core-level spectrum shows that the Sb atoms are bonded to only the top of Si atoms in a structure which has approximately one Sb atom per first layer Si atom. The core-level shifts associated with the different atoms of the Si(111)2×1 reconstruction are removed by the Sb overlayer, indicating that the Sb adsorption can be modeled as adatoms placed on an ideal unreconstructed Si(111)1×1 surface.

From SEXAFS, we find that each Sb atom is bonded to two Sb and two Si near neighbors. The surface bond lengths are close to those found in the bulk standards, Sb metal and crystalline AlSb. Polarization dependence of the Sb L_1 absorption near-edge structure shows that the Sb—Sb bonds are parallel to the surface plane. These SEXAFS findings show that Sb trimers occupy the threefold sites of the Si(111) surface, but, because neither a second-neighbor distance nor a second-neighbor coordination number could be determined, an unambiguous adsorption site determination is not possible from SEXAFS alone.

Fortunately, the geometric constraints obtained from photoemission combined with our intuition concerning bond lengths allow us to conclude that the Sb trimers occupy the threefold atop sites of the Si(111) surface. Apparently, it is the nondirectional close packing of co-

valent metallic atoms which leads to this high density structure.

By combining both photoemission and SEXAFS to the study of the same system, the interplay between surface electronic and geometric structure has been illustrated.

ACKNOWLEDGMENTS

This research encompassed the use of many different beamlines at NSLS. We thank each of the members of the individual participating research teams (PRT) for their help: R. McGrath, A. MacDowell, and P. Citrin of X15B, K. Tsang, R. Wood, and T. Rhodin of U16B, B. Katz and J. Kirkland of X23B, and P. Cowan and B. Karlin of X24A. We also thank C. Troxel of SSRL and R. Morris of the Stanford Electronics Laboratory for technical support. Useful discussion with L. Sorensen of the University of Washington is also appreciated. This research was supported by both the Stanford Synchrotron Radiation Laboratory and the National Synchrotron Light Source which are supported by the United States Department of Energy. This work was also supported by ONR and Defense Advanced Research Project Agency (DARPA) under Contract No. N00014-89-J-1083.

[1]D. H. Rich, G. E. Franklin, F. M. Leibsle, T. Miller, and T. C. Chiang, Phys. Rev. B **40**, 11 804 (1989).

[2]J. C. Woicik, P. Pianetta, and T. Kendelewicz, Phys. Rev. B **40**, 12 463 (1989).

[3]T. Kendelewicz, K. E. Miyano, R. Cao, J. C. Woicik, and W. E. Spicer, Surf. Sci. Lett. **220**, 726 (1989).

[4]T. Abukawa, C. Y. Park, and S. Kono, Surf. Sci. Lett. **201**, 513 (1988).

[5]R. A. Metzger and F. G. Allen, Surf. Sci. **137**, 397 (1984).

[6]D. Haneman, Rep. Prog. Phys. **50**, 1045 (1987).

[7]D. A. Shirley, Phys. Rev. B **5**, 4709 (1972).

[8]S. Doniach and M. Sunjic, J. Phys. C **3**, 285 (1970).

[9]F. Schaffler, R. Ludeke, A. Taleb-Ibrahimi, G. Hughes, and D. Rieger, Phys. Rev. B **36**, 1328 (1987); A. B. McLean, R. M. Feenstra, A. Taleb-Ibrahimi, and R. Ludeke, *ibid.* **39**, 12 925 (1989).

[10]M. P. Seah and W. A. Dench, Interface Anal. **1**, 2 (1979).

[11]*Table of Periodic Properties of the Elements* (Sargent-Welch Scientific Company, Skokie, Illinois, 1980).

[12]F. J. Himpsel, B. S. Meyerson, F. R. McFeely, J. F. Morar, A. Taleb-Ibrahimi, and J. A. Yarmoff, in *Photoemission and Absorption of Solids and Interfaces with Synchrotron Radiation,* Proceedings of the International School of Physics "Enrico Fermi," Proceedings of the Enrico Fermi School on "Photoemission and Absorption Spectroscopy of Solids and Interfaces with Synchrotron Radiation," Varenna, 1988 (North-Holland, Amsterdam, 1989).

[13]P. A. Lee, P. H. Citrin, P. Eisenberger, and B. M. Kincaid, Rev. Mod. Phys. **53**, 769 (1981).

[14]Ralph W. G. Wychoff, *Crystal Structures* (Wiley, New York, 1963).

[15]J. Stohr, R. Jaeger, G. Rossi, T. Kendelewicz, and I. Lindau, Surf. Sci. **134**, 813 (1983).

[16]F. Comin, P. H. Citrin, P. Eisenberger, and J. E. Rowe, Phys. Rev. B **26**, 7060 (1982).

[17]A. Kahn, Surf. Sci. Rep. **3**, 193 (1983).

[18]K. C. Pandey, Phys. Rev. Lett. **47**, 1913 (1981).

[19]J. C. Woicik, B. B. Pate, and P. Pianetta, Phys. Rev. B **39**, 8593 (1989).

[20]J. E. Northrup and M. L. Cohen, Phys. Rev. Lett. **49**, 1349 (1982).

[21]C. Y. Park, T. Abukawa, T. Kinoshita, Y. Enta, and S. Kono, Jpn. J. Appl. Phys. **27**, 147 (1988).

[22]J. J. Lander and J. Morrison, J. Appl. Phys. **36**, 1706 (1965).

[23]M. del Giudice, J. J. Joyce, and J. H. Weaver, Phys. Rev. B **36**, 4761 (1987).

[24]J. E. Rowe, in *Synchrotron Radiation Research: Advances in Surface Science,* edited by R. Z. Bachrach (Plenum, New York, 1990).

[25]W. A. Harrison, *Electronic Structure and the Properties of Solids* (Freeman, San Francisco, 1980).

[26]J. C. Woicik and P. Pianetta, in *Synchrotron Radiation Research: Advances in Surface Science,* edited by R. Z. Bachrach (Plenum, New York, 1990).

[27]P. H. Citrin, J. Phys. **47**, 437 (1986).

[28]J. Stohr and R. Jaeger, Phys. Rev. B **27**, 5146 (1983).